Atmospheric composition, radiative forcing, and climate change as a consequence of a massive methane release from gas hydrates

Gavin A. Schmidt and Drew T. Shindell

National Aeronautics and Space Administration (NASA) Goddard Institute for Space Studies and
Center for Climate Systems Research, Columbia University, New York, USA

Received 10 January 2002; revised 31 August 2002; accepted 14 October 2002; published 31 January 2003.

[1] The massive perturbation to global climate and the carbon cycle during the Paleocene/Eocene Thermal Maximum (PETM) (approx. 55.5 Ma) may have been forced by a catastrophic release of methane gas (CH_4) from hydrate deposits on the continental slope. We investigate whether reported PETM paleotemperature and paleo-CO_2 proxies are consistent with this hypothesis by considering the impact of large increases in CH_4 emissions to the atmosphere. Significant effects on atmospheric chemistry and CH_4 lifetime are seen for a range of plausible emission rates (1500 Gt carbon over 500–20,000 years). The resulting peak anomalous radiative forcing is 1.5–13.3 W/m^2 depending on the emission scenario. The scenarios most closely matched to the PETM carbon isotope excursion have peak forcing of around 3 W/m^2, which translates to peak temperature changes as a function of latitude that are a reasonable match to derived estimates. High CH_4 levels and enhanced stratospheric water vapor amounts persist for as long as do the emissions and are responsible for more of the peak radiative forcing than CO_2 levels, although results are sensitive to the background climate state and base CH_4 concentration. *INDEX TERMS:* 3337 Meteorology and Atmospheric Dynamics: Numerical modeling and data assimilation; 0322 Atmospheric Composition and Structure: Constituent sources and sinks; 3344 Meteorology and Atmospheric Dynamics: Paleoclimatology; 1610 Global Change: Atmosphere (0315, 0325)

Citation: Schmidt, G. A., and D. T. Shindell, Atmospheric composition, radiative forcing, and climate change as a consequence of a massive methane release from gas hydrates, *Paleoceanography*, *18*(1), 1004, doi:10.1029/2002PA000757, 2003.

1. Introduction

[2] The Paleocene/Eocene Thermal Maximum (PETM) event was characterized by extreme global warmth and a rapid, pronounced decrease (of up to −3‰ $\delta^{13}C$) in the mean carbon isotopic ratio of the global carbon cycle [*Kennett and Stott*, 1991; *Koch et al.*, 1992; *Katz et al.*, 1999; *Bains et al.*, 1999]. Deep ocean warming of about 4–6°C has been inferred in many cores. Estimates of surface warming from foraminiferal oxygen isotopes are from 5°C to 8°C in the high latitudes (ODP 690, Maud Rise, South Atlantic, ≈65°S), 1–4°C in the subtropics (DSDP 527, Walvis Ridge, South Atlantic, ≈35°S), and 1–2°C in lower latitudes (ODP 1051, Blake Nose, North Atlantic, ≈30°N, ODP 865, Allison Guyot, Equatorial Pacific, ≈18°N) [*Bralower et al.*, 1997; *Bains et al.*, 1999; *Thomas et al.*, 1999].

[3] A compelling explanation for the carbon isotope excursion is a massive release of methane gas (CH_4) from hydrates along continental margins [*Dickens et al.*, 1995]. Although the amount and duration of this CH_4 input remains poorly constrained, current literature suggests approximately 1500–2000 Gt of carbon (1 Gt = 10^{15} g) over 10–20 kyr was added to the system [*Röhl et al.*, 2000; *Dickens*, 2001]. However, a number of important questions remain open. In particular, was the contemporaneous global warming driven by this release, or were prior climate changes the initiator of the event? [*Katz et al.*, 2001; *Bice and Marotzke*, 2002]. Additionally, was this CH_4 injected and oxidized directly into the ocean or did it bubble up into the atmosphere? [*Dickens*, 2000]. Recently reported research using single specimen isotopic analyses of foraminifera at ODP 690 has indicated that the changes in both carbon and oxygen isotopes were earlier and faster at the surface than at intermediate or deeper depths [*Zachos et al.*, 2001]. Thus, at least at this location, the anomalous warmth and carbon isotope excursion appear to be synchronous and likely occurred first in the atmosphere. This is consistent with CH_4 emissions directly into the atmosphere and some degree of consequential global warming.

[4] In the present-day atmosphere, CH_4 is rapidly oxidized to carbon dioxide (CO_2), and has a lifetime of about 10 years [*Prather et al.*, 2001, and references therein] Thus, it has generally been assumed that any direct radiative forcing from changes to the atmospheric CH_4 concentration would have been minimal, and that any climate perturbations were driven primarily by the increases in CO_2 [*Dickens*, 2000]. However, consideration of atmospheric chemistry implies that the residence time for CH_4 will be significantly augmented as concentrations increase [e.g., *Sze*, 1977; *Isaksen and Hov*, 1987; *Prather et al.*, 2001] through a feedback that reduces the abundance of atmospheric OH radicals, the dominant chemical sink. There will also be greater CH_4 oxidation in the stratosphere (an important source of stratospheric water vapor, H_2O_{str}), and it has been suggested that amounts of polar stratospheric clouds may

0883-8305/03/2002PA000757$12.00

increase [*Sloan et al.*, 1992; *Sloan and Pollard*, 1998]. Although the feedback of CH_4 on its own lifetime has been previously considered in this context [*Sloan et al.*, 1999; *Peters and Sloan*, 2000; D. Hammond, personal communication] we attempt to better quantify this effect and its climatic consequences here.

[5] Our knowledge of the atmospheric composition and climate during the Paleocene are highly uncertain. Estimates for the base CO_2 level range from 300 to 2000 ppm [*Sinha and Stott*, 1994; *Royer et al.*, 2001; *Pearson and Palmer*, 2001], while for CH_4 a range of 7–10 ppm has been estimated based on a threefold increase in wetland areas (compared to the present-day) during this period [*Sloan et al.*, 1992, 1999]. Increased tectonically driven sources have also been proposed [*Hudson and Magoon*, 2002]. Estimates of concentrations during the PETM event itself are either not available or very poorly constrained [*Sinha and Stott*, 1994]. These uncertainties have relevance to the fate of any anomalous CH_4 emissions in two principle ways; the effect of base CH_4 level on the oxidation capacity of the atmosphere, and the effect of warming from all greenhouse gases (GHGs) on the surface climate. Atmospheric chemistry is not affected directly by the level of CO_2, which is, for these purposes, chemically inert.

[6] In light of these difficulties, we principally consider perturbations to the better understood preindustrial (ca. 1850) atmosphere. Ice core data provide accurate preindustrial CH_4 concentrations and we have reasonable estimates of natural emissions of the important gases. Crucially, we know that atmospheric CH_4 was roughly in steady state, and that therefore the sources and sinks were balanced. This allows us to then close the budget for CH_4. In the text below, we discuss the impacts of different atmospheric concentrations wherever relevant.

[7] Starting with a number of CH_4 emission scenarios for the PETM consistent with the observed carbon isotopic excursion, we simulate the atmospheric chemistry response and the subsequent radiative forcing by increased GHGs (i.e., CH_4, CO_2, and H_2O_{str}). We then use a atmospheric general circulation model (GCM) to estimate the degree of consequential surface warming and, by comparing the results with the inferred climate change, we attempt to constrain possible emission scenarios.

2. Atmospheric Chemistry Modeling

2.1. Model

[8] In order to estimate atmospheric chemistry changes over the tens of thousands of years relevant for the PETM, we require estimates of the feedback between CH_4 and OH when CH_4 concentrations are high. We start with a two-dimensional (2-D) atmospheric chemistry model based on the 3-D tropospheric and stratospheric chemistry used in the Goddard Institute for Space Studies (GISS) GCM [*Shindell et al.*, 1998, 2001a; *Shindell and Grewe*, 2002], with photochemical reaction rates updated to the most recent estimates [*Sander et al.*, 2000]. The tropospheric component uses HO_x-NO_x-O_x-CO-CH_4 chemistry (Figure 1), neglecting higher hydrocarbons (with the exception of isoprene, which is included as the equivalent amount of CO). In this 2-D version, water vapor is taken from the GCM mean fields (for present-day climate), while CO is held fixed. It also includes NO_x emissions from soils, biomass burning, and lightning and parameterized hydrologic removal of soluble gases derived from the full GCM, providing a crude approximation of global behavior.

[9] The increase in CH_4 lifetime as concentrations increase is due to the exhaustion of OH radicals, which are the primary tropospheric oxidizing agents [*Levy*, 1971]. The schematic in Figure 1 shows the basic features of tropospheric oxidation chemistry. The full chemistry scheme involves many more reactions than are shown here (for instance there is a long oxidation chain between CH_4 and the final product CO_2). Including all the steps and the intermediate products would unnecessarily increase the complexity of the diagram. Further details can be found in the cited references if required.

[10] The essential elements (going clockwise around the figure) can be outlined as follows: (1) NO and NO_2 can be considered to be in equilibrium, (2) photolysis of NO_2 is a source of atomic oxygen, which rapidly combines with molecular oxygen to form O_3 (although there are also important stratospheric sources of both O_3 and NO_2), (3) the destruction of O_3 in turn by UV radiation provides the principle source of OH (via the reaction of excited singlet D oxygen atoms with water), (4) OH and HO_2 can also be considered in equilibrium, (5) OH is converted into HO_2 during oxidation of CH_4 (and CO or higher hydrocarbons), and (6) the reaction of HO_2 with NO is the primary pathway that regenerates both NO_2 and OH. There are important sources for NO_2 from surface emissions, lightning and transport from the stratosphere, and sinks for NO and NO_2 by rain-out of HNO_3, for HO_2 again by rain-out via hydrogen peroxide (H_2O_2) and for tropospheric ozone by dry deposition (which also removes NO and NO_2).

[11] With increases in hydrocarbons (such as CH_4, but also isoprene and CO, which play a similar role) the limiting factor in the recycling of OH is the concentration of NO. This is thought to be the limiting step throughout most of the present-day atmosphere, even with large emissions of NO and NO_2 from fossil fuel burning and CH_4 emissions much less than at the PETM. With large CH_4 amounts, the equilibrium between OH and HO_2 moves toward higher HO_2 amounts. While this in turn pushes the NO/NO_2 balance toward NO_2, enhancing OH production via ozone, this is outweighed by a shift toward HO_2. Additionally, the hydrogen peroxide sink for the HO_2 radical acts more efficiently, which further draws down OH levels.

[12] With increased CH_4 emissions, tropospheric oxidation thus becomes less effective, and the other principal sinks for CH_4 (stratospheric oxidation, and the poorly constrained soil sink) will grow in importance. This will in turn lead to higher H_2O_{str} amounts. To account for stratospheric changes impacting on the troposphere (through changes in UV absorption which plays a role in tropospheric OH production, and in sources for NO_2 and O_3), we also include linearized stratospheric chemistry. This allows the first-order feedbacks between CH_4, H_2O_{str} and stratospheric O_3 to be estimated [*Shindell and Grewe*, 2002]. The chemistry is linearized around a base preindus-

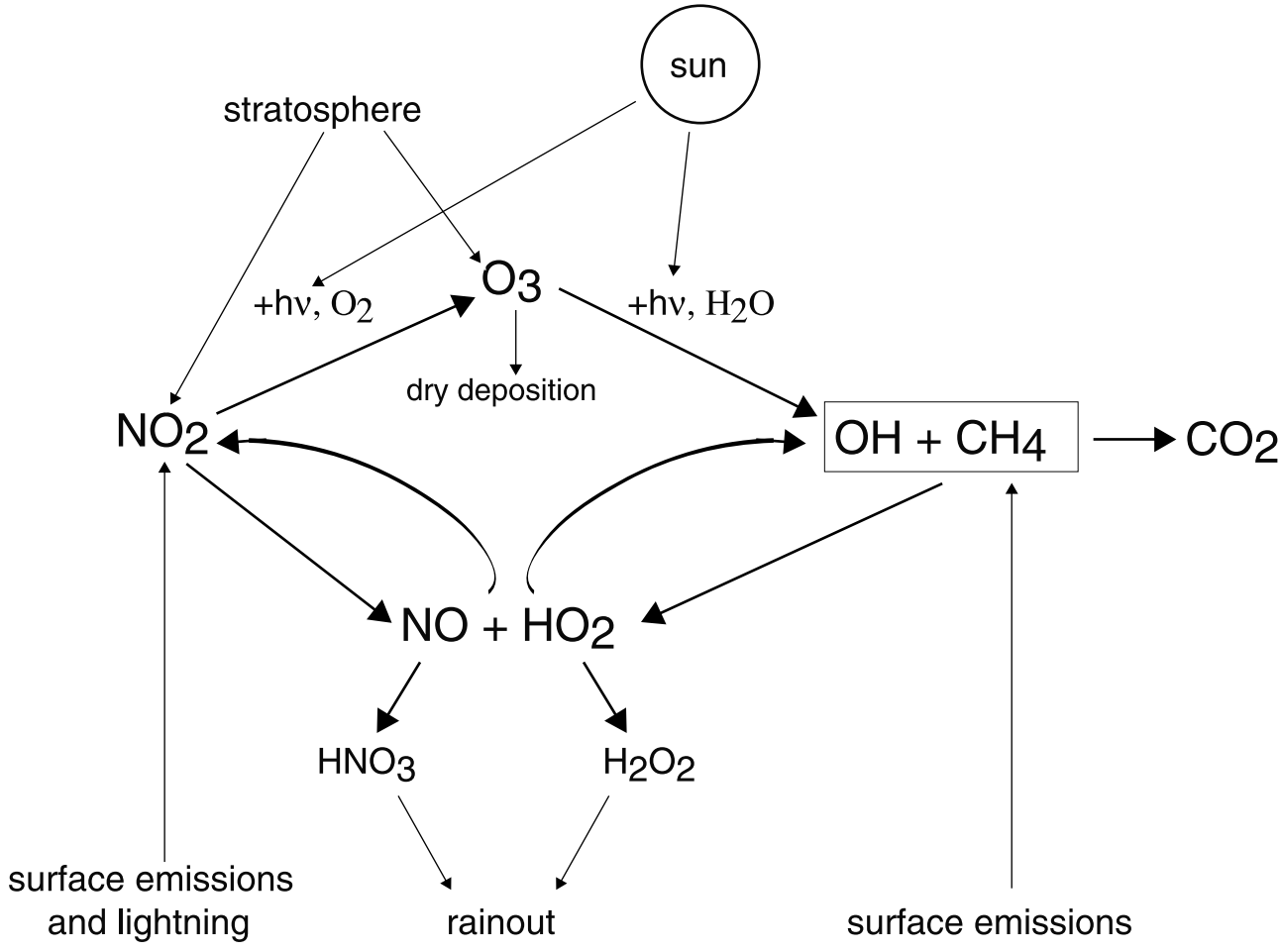

Figure 1. Simplified schematic of the tropospheric chemistry scheme, showing the primary pathways for OH radical generation and loss. For clarity, some intermediate reactions and the effects of CO and higher hydrocarbons are not shown. Increases in CH_4 decrease the OH/HO_2 ratio and also increase the sink of HO_2 via H_2O_2 (see text for details).

trial atmospheric composition, and the tendencies in O_3 due to temperature, H_2O_{str}, and UV radiation are calculated. The chemistry model thus contains the main processes that determine OH abundances, and reproduces the present-day oxidation capacity seen in the full 3-D simulation. Note that the full stratospheric water budget is highly uncertain and will be greatly impacted by changes in, for instance, tropopause temperatures and tropospheric–stratospheric exchange dynamics. Thus in this paper, we consider only the forced change in H_2O_{str} due to increased CH_4 oxidation, and not any feedbacks that could depend on the subsequent climate change.

[13] The sensitivity of the 2-D model compares well to more complicated models. For instance, the change in the OH sink (considering the tropospheric chemistry response only) for a 10% increase in CH_4 over present-day amounts is −2.8%, compared to a range of −2.9% to −3.5% for a selection of 3-D chemical transport models [*Prather et al.*, 2001, Table 4.3, p. 251]. Including the linearized response of stratospheric ozone to temperature, humidity, and UV (but not to changes in ozone transports), leads to an additional negative feedback. Increasing CH_4 leads to increasing H_2O_{str}, a small decrease in stratospheric O_3, and an increase in the amount of UV reaching the troposphere, consequently increasing the photolytic production of OH radicals. This is however a small effect, reducing the OH change by about 0.2% to −2.6%.

[14] In the Paleocene, warmer temperatures will have likely lead to increased atmospheric water amounts that affect the production of OH. An estimate of H_2O increases in a greenhouse world would be about 30% for a 4°C temperature increase, making the reasonable assumption that relative humidity is roughly constant [*IPCC*, 2001]. Over a range of GCM experiments, the increase in OH for this magnitude change is less than 10% [*Grenfell et al.*, 2001, personal communication]. This actually leads to an increased sensitivity to CH_4 changes, though not by a significant amount. Another unknown quantity at this time is the amount of higher hydrocarbons emitted from vegetation whose distribution was likely to have been more

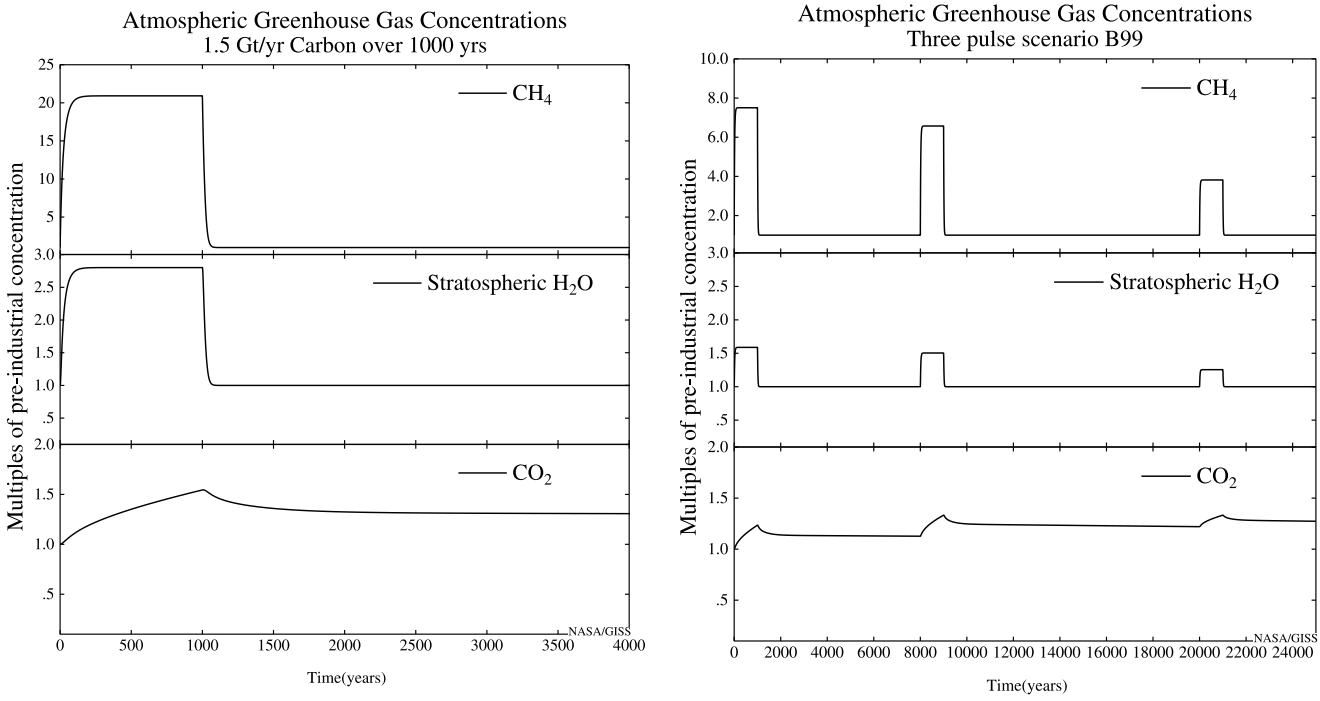

Figure 2. Selected transient scenarios for large CH_4 releases based on 2-D chemistry model estimates of the tropospheric sink and the transient equations outlined in the text. Other uniform scenarios resemble the first panel.

extensive than at present. Increases in these emissions would reduce the atmospheric oxidation capacity and lead to higher CH_4 concentrations.

2.2. Results

[15] The change in OH amounts and CH_4 residence time for a series of CH_4 concentrations are outlined in Table 1. The change in oxidation capacity can be characterized by the percentage decrease in OH concentration or by the relative specific loss term for CH_4. For example, a 10% decrease in OH, leads to a relative specific loss of 0.9 compared to the control. In the absence of any nonlinear feedback on CH_4 oxidation, the relative specific loss would be identically one (i.e., the loss rate would simply be proportional to the concentration). Thus, a smaller relative specific loss implies a greater nonlinear reduction in tropospheric oxidation.

[16] We calculated the OH change for CH_4 concentrations from 0.7 to 140 ppmv (200 times preindustrial values). The results show an exponential decline in oxidation capacity as CH_4 increases (in the absence of any other changes). Note that the preindustrial to present-day concentration change (M = 2.5, concentrations going from 0.7 to 1.75 ppmv) gives an almost 20% decline. However, in the real climate concomitant increases in NO_x emissions and tropospheric O_3 have had an opposing effect.

[17] We also present the changes in O_3 from the linearized stratospheric chemistry. Increasing H_2O_{str} amounts lead to generally less ozone, but lower temperatures (due to increased radiative cooling) tend to increase ozone. These estimates should be considered tentative due to the large number of processes important for O_3 not included here.

[18] Transient concentration changes (for CH_4, CO_2, and H_2O_{str}) given various emission scenarios are then calculated using a basic two-box (troposphere and stratosphere) model (described in Appendix A) using the chemistry results as a look-up table (Figure 2). This approach has the advantage of producing reasonable long-term estimates, but obviously neglects any feedbacks between the climate changes driven by the GHGs and the chemistry. Also, any important feedbacks from global warmth on the background CH_4 or CO_2 emissions will not be included. These feedbacks could include the response of wetlands to temperature/precipitation changes, or from alterations to the ocean carbon cycle. Given the size of these imposed perturbations, however, we

Table 1. 2-D Atmospheric Chemistry Calculations[a]

CH_4 M	OH (% Change)	Relative Specific Loss Rate (S_{trop})	CH_4 Lifetime (years)	ΔO_{3strat} (% Change)
1	0.0	1.0	8.4	0
2.5	−19.2	0.808	10.1	−9
4	−30.8	0.692	11.5	−15
7	−42.5	0.575	13.4	−19
10	−56.5	0.435	16.7	−23
40	−78.1	0.219	26.9	−26
100	−90.4	0.096	41.1	−3
200	−91.2	0.088	42.5	+10

[a]The concentration M is the multiple of the preindustrial CH_4 concentration (0.7 ppmv). The OH radical variation is given as a percentage increase over the preindustrial climate. The relative specific loss is the fractional change to the tropospheric sink term for CH_4 compared to the preindustrial control. The lifetime for CH_4 is defined with respect to the total source term. The ozone change figures are zeroth-order estimates from the 2-D chemistry model but do not include any advective effects.

Table 2. Concentration of Forced GHGs and Radiative Forcing[a]

	Atmospheric Concentration Increase (ppmv)			Radiative Forcing (W/m^2)[b]		
Experiment	CO_2	CH_4	H_2O_{str}	CO_2	$CO_2 + CH_4$	All
3 Gt/yr (500 years)	200	47.2	15.9	3.3	11.4	13.3
1.5 Gt/yr (1 kyr)	160	14.9	5.0	2.7	6.2	7.2
0.3 Gt/yr (5 kyr)	100	1.8	0.6	1.9	2.6	2.8
0.15 Gt/yr (10 kyr)	90	0.8	0.3	1.8	2.2	2.2
0.05 Gt/yr (10 kyr)[c]	30	0.2	0.1	0.7	0.8	0.8
B99 (transient)	90	3.6	1.2	1.8	3.0	3.3

[a]All concentrations are given as ppmv increases over preindustrial values (280, 0.7, and 2.6 ppmv, respectively). Values given correspond to the time of maximum CH_4. Maximum CO_2 levels occur a few years later but do not differ substantially. For the B99 experiment, we highlight the equilibrium concentrations at the end of the second pulse. "All" radiative forcing includes the increases in CO_2, CH_4, and H_2O_{str}.

[b]The radiative forcing is the instantaneous response at the tropopause to an increase to the GHG concentrations at the end of the release period compared to a preindustrial control run.

[c]In the 0.05 Gt/yr case, ocean oxidation of 0.10 Gt/yr CH_4 will lead to an increased air–sea flux of CO_2, an estimated peak concentration increase 30–40 ppmv higher than calculated, and an extra forcing of about 0.7 W/m^2.

anticipate that the procedure outlined here will serve to produce reasonable first-order estimates of the changing concentrations.

[19] We choose to input a constant total CH_4 amount (equivalent to 1500 Gt of carbon) representative of the PETM in a number of ways in order to bracket the possible responses. First, we calculate the transient scenarios assuming a large, short-term pulse (uniform over 500 years). Note that even if the CH_4 release were effectively instantaneous, the equations predict that it would be over 200 years before CH_4 levels came close to their previous value. Second, we consider a number of more gradual releases over 1000, 5000, and 10,000 years (1.5, 0.3, and 0.15 Gt/yr, respectively). Detailed analysis of the PETM carbon isotope excursion [*Bains et al.*, 1999] suggests that the initial decrease occurred in three distinct steps over 20,000 years, each corresponding to an input of about 600, 500, and 300 Gt of carbon within about 1000 years. The transient scenario B99 simulates this hypothesized three pulse release (scaled so that the total input is 1500 Gt). Finally, we consider the response of the atmosphere to a gradual release, but with two-thirds of the CH_4 oxidized in the deep ocean, leaving only a 0.05 Gt/yr emission over 10,000 years directly into the atmosphere. The results for the various scenarios are summarized in Table 2.

[20] For scenarios with pulses longer than a few hundred years, CH_4 concentrations stabilize since the timescale for the change in emissions is now significantly longer than the atmospheric residence time (Table 1). However, CO_2 levels will continue to increase until the emissions cease (since the residence time for CO_2 is considerably longer).

[21] With the exception of the 500 year pulse experiment, CO_2 levels do not rise substantially (160 ppmv at maximum and less than 100 ppmv for the B99 case). For comparison, *Dickens* [2000] estimates an eventual rise of about 60 and 85 ppmv in atmospheric concentrations for two cases where all CH_4 would be completely oxidized in the ocean, or atmosphere, respectively. That study assumed an input of 840 Gt carbon over 10,000 years. With the larger source function used here (1500 Gt), we estimate that this would translate to peak increases of about 100 and 150 ppmv instead. The 150 ppmv figure can be compared directly to the 90 ppmv increase predicted for the 0.15 Gt/yr experiment in Table 2. The difference is due to the details of the carbon cycle model used in the previous study, rather than the slower oxidation rate assumed due to the CH_4 feedback. This therefore gives some idea of the uncertainty in the CO_2 calculations.

[22] In the case where we assume that two-thirds of the CH_4 is oxidized in the ocean, there will be an increased air–sea flux of CO_2 to the atmosphere, which is not accounted for in our model. Judging from the results of *Dickens* [2000], we estimate that this would reduce the total atmospheric concentration increase by about a quarter (compared to full atmospheric oxidation). We would therefore be missing around 30–40 ppmv CO_2 giving a peak increase of around 70 ppmv. However, this is a rather unsatisfactory estimate, and would be better examined in a model with a full carbon cycle.

[23] Note that in all cases, the increases in CO_2 are independent of the assumed background concentration (within a few ppmv). However, this is not true for CH_4 (and hence H_2O_{str}) due to the nonlinearities in the chemistry. A hypothesized threefold increase in natural CH_4 sources due to enhanced wetland areas [*Sloan et al.*, 1999] would lead, using our model, to a base CH_4 level of 2.9 ppmv (see Appendix A for details). Since there may also have been other extra sources of CH_4 [*Hudson and Magoon*, 2002], and also other hydrocarbons, we consider the sensitivity of our results assuming a "Paleocene" value of 6 ppmv (and consequent concentration of H_2O_{str} of 4.4 ppmv). The increase in CH_4 concentrations due to anomalous emissions, assuming this base level, are larger than for the preindustrial case, ranging from a further increase of 0.4 ppmv (0.05 Gt/yr case) to 22 ppmv (500 year pulse). The B99 experiment would have an additional increase of 2.4 ppmv over the value shown in Table 2.

3. Radiative and Climate Forcing

[24] Estimates of radiative forcing are a useful way to characterize the climate response to changes in GHG amounts. For well-mixed gases (such as CO_2 or CH_4), the instantaneous forcing at the tropopause (i.e., the change in the net radiative flux if GHG concentrations are instantly increased) has been shown to be a good predictor of subsequent climate change across a range of models and scenarios [*IPCC*, 2001]. The instantaneous forcing for H_2O_{str} is not quite as useful because of the changes to the forcing that occur as stratospheric temperatures adjust to the new water vapor concentration. In this case the "adjusted forcing," where stratospheric (but not tropospheric) temperatures are allowed to come into equilibrium, is a better predictor [*Hansen et al.*, 1997b]. However, this difference is only around 10% [*Oinas et al.*, 2001], and is therefore neglected in the rest of this discussion.

[25] We used the GISS radiative transfer model [*Lacis and Oinas*, 1991], as implemented within the GISS GCM, to compare the climate forcing from the GHG concentration changes from Table 2. The radiative transfer code uses 33

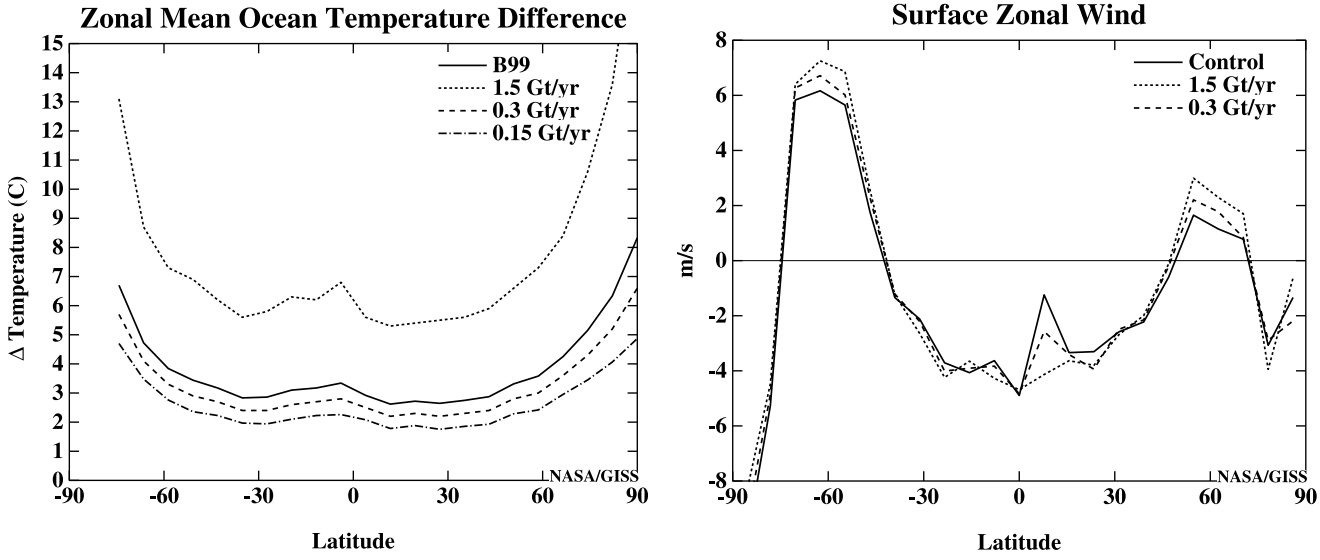

Figure 3. (a) Equilibrium zonal mean annual average surface ocean temperature difference from the control and (b) surface zonal winds from GCM simulations using the CH_4 and CO_2 concentrations from scenarios described in Table 2.

separate spectral intervals to give results that are in good agreement with more detailed line-by-line calculations [*Oinas et al.*, 2001].

[26] The forcing from each scenario due to CO_2 alone, CO_2 and CH_4 together, and total forcing including H_2O_{str} are given in Table 2. For comparison, a doubling of CO_2 in this model (from 280 to 560 ppmv) produces an instantaneous change in forcing of 4.4 W/m^2 at the tropopause. The radiative forcing for CO_2 is roughly proportional to the logarithm ($\approx$4.4log(C)/log(2)) of its concentration while for CH_4, the forcing scales like the square root [*IPCC*, 2001]. This implies that the higher the base level, the smaller the forcing will be from a fixed increase in concentration.

[27] The results in Table 2 show the increased radiative forcing with respect to a simulation with preindustrial GHG concentrations. Note that the peak concentrations and forcing for the B99 case are taken from the end of the second pulse. In all cases, a large part of the forcing is due to the CH_4 increase, and even in the smaller input experiments, the CH_4 plus H_2O_{str} forcing is almost equal to that of CO_2 alone. CO_2 dominates the forcing only in the case where most CH_4 was oxidized in the ocean (especially if you take account of the possibly increased air–sea flux discussed above).

[28] With estimated Paleocene base levels (6 ppmv CH_4), the ppmv increases for the same anomalous CH_4 emissions are higher (since the residence time of CH_4 is longer). However, the anomalous forcing will be less. For instance, the B99 forcing due to CH_4 would be decreased 20% despite an additional increase of 2.4 ppmv due to the higher CH_4 base level. This effect is even more important for CO_2 and, if the highest estimates for the Paleocene concentration are correct, imply that the radiative forcing from the modeled CO_2 increases here would be around 50% less. The total difference this makes for the 500 year pulse is very small, but the decrease in total forcing for the 1.5 Gt/yr, 0.3 Gt/yr, and B99 experiments are 7%, 28%, and 24%, respectively.

[29] For any particular climate model, the response of the climate will be well approximated by the radiative forcing multiplied by that model's climate sensitivity. For present-day climate simulations, the sensitivity ranges from roughly 0.5°C/(W/m^2) to 1°C/(W/m^2) depending on the climate model used [*IPCC*, 2001]. Thus a 3 W/m^2 forcing would translate to a global mean surface temperature change of between 1.5°C and 3.0°C.

[30] The change in latitudinal temperature gradient is more model dependent. In order to make a first-order estimate, we ran a coarse resolution (8° × 10°) version of the GISS middle atmosphere GCM (model top at 85 km) with a mixed layer ocean and thermodynamic-only sea ice [*Shindell et al.*, 2001b]. This model assumes fixed ocean heat transports but allows ocean temperatures to adjust to the radiative forcing (which takes about 20 or 30 model years). It also has a resolved stratosphere which has been shown, in particular, to affect the sensitivity of zonal winds to GHG forcing [*Shindell et al.*, 1999]. We used present-day boundary conditions (continental configurations, soil, vegetation, and ice sheets) to allow an easy comparison between these results and other climate models.

[31] We ran the model with the stabilized concentrations of CH_4 and CO_2 from the 1.5 and 0.3 Gt/yr scenarios and compared the results to a preindustrial control run. The last 30 years of a 60 year simulation were used to examine the new equilibria. As expected, the global mean temperature changes, 6.7°C and 2.9°C, respectively, are proportional to the radiative forcing (implying a climate sensitivity of about 1°C/(W/m^2)). Equilibrium temperature responses for all of the scenarios (and including the additional H_2O_{str} forcing) can therefore be estimated by scaling these results to the total radiative forcing outlined in Table 2.

[32] Figure 3a shows the change in zonal mean ocean temperature for various scenarios. There is a clear high latitude amplification due to snow and sea ice feedbacks on

the albedo. Tropical warming is significantly less but still substantial and the equator-to-pole temperature gradient is decreased. These results are similar to most GHG forced simulations for the present-day, with the minor caveat that the climate sensitivity of this model is higher than most (at the other extreme, for instance, the NCAR CSM has a sensitivity closer to 0.5°C/(W/m^2)). Model simulations using Paleocene/Eocene boundary conditions are generally warmer (due to the absence of continental ice and changes in vegetation albedo). However, the sensitivity of these simulations to increased GHG forcing is very similar to that under present-day boundary conditions [*Sloan and Rea*, 1995; *Sloan and Pollard*, 1998; *Huber and Sloan*, 2001]. In particular, all existing simulations show high latitude amplification of the temperature response even at very high GHG amounts (up to at least 6 times CO_2), despite having less sea ice and snow covered area. This response is thus likely to be ubiquitous except in the extreme case of a complete absence of seasonal sea-ice or snow cover. The temperature results seen here can therefore be assumed to be roughly representative of model responses to increased GHG amounts both for the present-day and in the Paleocene.

[33] One particularly noticeable feature, different to some previous simulations of warm climates, is that surface zonal winds increase (Figure 3b) [see also *Rind et al.*, 2001]. This is related to stratospheric radiative cooling and strengthening of the winter polar vortex, which leads in turn to significantly lower polar pressures and enhanced zonal winds in the lower stratosphere which project all the way down to the surface. This drives an increased westerly circulation pattern similar to that seen in anthropogenic climate warming scenarios [*Shindell et al.*, 1999, 2001b] which enhances regional temperature increases in continental interiors.

4. Discussion

[34] Can these simple experiments help constrain the uncertainties associated with the CH_4 release hypothesis for the PETM? First, we can say something concerning the necessary total radiative forcing required to match the inferred temperature changes. The surface temperature changes seen in the B99 or 0.3 Gt/yr experiments match the peak observed changes in the high latitudes relatively well (5–7°C), but warm more than observed (2–3°C) in the tropics. Within the uncertainty of the data (due to diagenetic effects, changes to the seawater $^{18}O/^{16}O$ ratio, etc. (see the study of *Crowley and Zachos* [2000] for a fuller discussion)) and the incompleteness of the model (poor tropical resolution, no changes in ocean heat transports, etc.), we feel that this order of magnitude forcing (around 3 W/m^2) is likely to have been necessary to produce the observed shifts. If the real world climate sensitivity is significantly less than in the model used here (say 0.5 compared to 1°C/(W/m^2)) then the forcing would need to be doubled for a similar temperature response.

[35] If forcing of 3 W/m^2 were to be supplied purely from CO_2 increases, that would require a 60% increase over the base concentrations (and if twice as much forcing were required, up to 2.6 times base CO_2 levels would be necessary). These kinds of increase (at minimum 170 ppmv for the preindustrial base level, and 340 ppmv for a base climate with 560 ppmv), are much larger than can be accounted for from the direct effects of full oxidation of any anomalous CH_4 emissions. Therefore either the CH_4 emissions were much larger (though this is inconsistent with the magnitude of the carbon isotope excursion [*Dickens et al.*, 1995; *Dickens*, 2000]) or a source of radiative forcing other than CO_2 must have been present during the PETM.

[36] Our working hypothesis is that some of the CH_4 was emitted directly into the atmosphere. In order to match the forcing, these emissions likely exceeded 0.3 Gt/yr (at least for some multicentennial interval). More rapid emissions (such as in the 500 year pulse experiment) produce too strong a forcing, and do not persist long enough to sustain the higher surface temperatures. On the other hand, slower emissions (such as the 0.15 Gt/yr experiment) last long enough, but probably do not provide enough forcing.

[37] In order for the deep sea to have warmed as much as inferred from the benthic foraminiferal results (about 4°C) the forcing must have continued for a few thousand years (long enough for the heat to have been diffused or advected into the deep ocean). Although, a faster response ($\ll$1 kyr) due to a switch in location of deep water formation is also possible [*Bice and Marotzke*, 2002]. The return to background values in the deep ocean will take a similar length of time once the anomalous radiative forcing is removed. Since the scenarios explored here have forcings decreasing after a maximum of 25,000 years (i.e., for B99), this implies that that peak deep ocean temperatures will only last for a few thousands of years longer (in the absence of any oceanic or terrestrial feedbacks that might prolong the CO_2 excursion). This seems consistent with the period of peak benthic warmth seen in ODP 690 of a few tens of thousands of years within a total excursion of around 120,000 years [*Norris and Röhl*, 1999].

[38] The length of the forcing and its magnitude seen in the 0.3 Gt/yr and B99 experiments therefore seem qualitatively sufficient to match the observations. Note that, due to the nonlinearity of the CH_4 lifetime response, the peak radiative forcing in a pulsed release will be significantly higher than for a more uniform emission (however, the long-term mean forcing is dependent on the exact characteristics of the pulsing). While we note the substantial uncertainties in data interpretation, climate sensitivity, base climate state, and atmospheric composition, we nevertheless conclude that a massive CH_4 release from the dissociation of gas hydrates can consistently explain the PETM climate change. However, should future analyses lead to a substantial prolonging of the period of deep ocean warmth over that assumed above, these conclusions may have to be revisited.

[39] There are many feedbacks, not considered in this study, which will need to be accounted for in future work. For instance, we have neglected temperature and humidity effects on atmospheric reaction rates, productivity changes on the uptake of carbon [*Bains et al.*, 2000; *Beerling*, 2000], changes in ocean temperatures and mixing [*Bice and Marotzke*, 2002], and variations in the rate of stratospheric–tropospheric exchange. We also neglected the highly uncertain effects of possible increases in polar strato-

spheric clouds [*Sloan and Pollard*, 1998]. Stratospheric temperature and H_2O_{str} changes affect ozone amounts, but thoroughly estimating those changes and subsequent radiative effects are beyond the scope of this paper. Given the size of the CH_4 source function, we anticipate that these effects may well be important (especially over the longer term). Whether these feedbacks are strong enough to change the conclusions presented here, however, remains to be seen. Work also remains to be done to link the atmospheric chemistry to a more sophisticated carbon cycle model [e.g., *Dickens*, 2000, 2001].

[40] In conclusion, through changes in the tropospheric chemical sink of CH_4, the radiative consequences of a massive CH_4 release from gas hydrates are significantly enhanced over that previously assumed. Although CH_4 and H_2O_{str} have residence times significantly shorter than CO_2, they will persist at high concentrations for as long as anomalous emissions last. We have been able to reconcile global warmth at the PETM without significant (>100 ppmv) CO_2 increases. Predicted changes to CO_2 are small compared to the sensitivity of standard proxies, and underline the difficulty in detecting possible increases across the PETM interval.

Appendix A. Simple Two-Box Model

[41] Assuming CH_4 and CO_2 are well mixed in the troposphere allows us to construct a simple two-box model for the mean concentrations of CH_4, CO_2, and H_2O_{str} (at least the CH_4-related portion). We assume that natural sources exactly balance the preindustrial (ca. 1850) sinks, with a preindustrial residence time for CH_4 (τ_M = total reservoir divided by the source) of 8.4 years. We define α as the tropospheric fraction of the total preindustrial sink. The variation of this chemical sink as the CH_4 concentration varies is written as S_{trop} and is approximated from the results in Table 1. The stratospheric sink is a photolytic reaction and is presumed proportional to the concentration, as is the biological soil sink. In the preindustrial, we estimate the tropospheric, stratospheric and soil sinks to be 88%, 7%, and 5% of the total sink, respectively (i.e., α = 0.88), consistent with the 2-D modeling results and the magnitude of the present-day sinks [*Prather et al.*, 2001].

[42] We define the mean stratosphere to be above 200mb. From present-day observations of the stratospheric CH_4 sink (about 40 Tg/yr), the residence time for stratospheric air (about 5 years), and the mass of the stratosphere ($\approx 10^{18}$ kg), we estimate the fraction of CH_4 crossing 200mb that is oxidized to be $\lambda = 0.21$. Due to freezing out of some H_2O_{str}, its residence time (τ_W) is slightly shorter than that of stratospheric air by a factor μ, assumed here to be 0.8.

[43] We define M, W, and C as the multiples of the preindustrial mixing ratios of CH_4, H_2O_{str}, and CO_2, respectively. Their evolution can be expressed as

$$M_t = \left(1 - \left[\alpha S_{trop} + (1-\alpha)\right]M\right)\tau_M + I(t)$$

$$W_t = (1 - W + 2\mu\lambda(M-1)M_0/W_0)/\tau_W$$

$$C_M(t) = (M_0/C_0)\left(\alpha S_{trop} + (1-\alpha)\right)M)/\tau_M$$

where I is the input function of CH_4, and M_0, C_0, and W_0 are the estimated preindustrial atmospheric mixing ratios (0.7, 280.0, and 2.6 ppmv, respectively). $C_M(t)$ is defined as the source of CO_2 at any point in time. Atmospheric concentrations of CO_2 are calculated following a multiple timescale decay [*Lashof and Ahuja*, 1990] with the longest timescale set to 100,000 year to match the decay time for the PETM carbon isotope excursion [*Bains et al.*, 1999].

[44] The increase in H_2O_{str} purely due to increasing CH_4 since the preindustrial is estimated to be about 0.34 ppmv, in line with more detailed model estimates. At any point where M is in equilibrium with the anomalous emissions I, the new residence time for CH_4 can be calculated as $\tau'_M = \tau_M/(\alpha S_{trop}(M) + 1 - \alpha)$. For reference, a threefold increase in surface emissions [*Sloan et al.*, 1999] leads to M_0 = 2.9 ppmv, α = 0.78, a CH_4 residence time of 11.6 years and a base H_2O_{str} level of 3.3 ppmv. If a Paleocene value of 6 ppmv is assumed (which would require a roughly fivefold increase in emissions), the CH_4 residence time would be 15 years and the base H_2O_{str} level, 4.4 ppmv.

[45] The coding of the two-box model that was used to generate the results reported here is available at http://www.giss.nasa.gov/gavin/petm.html.

[46] **Acknowledgments.** We would like to thank Greg Faluvegi for running some of the radiative forcing calculations, Bernadette Walter and Francesco Tubiello for advice concerning the carbon and CH_4 cycle, Jerry Dickens and Matthew Huber for some very constructive criticism, and Doug Hammond, Lisa Sloan, and an anonymous reviewer for generously sharing their thoughts on this subject with us.

References

Bains, S., R. M. Corfield, and R. D. Norris, Mechanisms of climate warming at the end of the Paleocene, *Science*, *285*, 724–727, 1999.

Bains, S., R. D. Norris, R. M. Corfield, and K. L. Faul, Termination of global warmth at the Palaeocene/Eocene boundary through productivity feedback, *Nature*, *407*, 171–174, 2000.

Beerling, D., Increased terrestrial carbon storage across the Palaeocene–Eocene boundary, *Palaeogeogr. Palaeoclimatol. Palaeoecol.*, *161*, 395–405, 2000.

Bice, K. L., and J. Marotzke, Could changing ocean circulation have destabilized methane hydrate at the Paleocene/Eocene boundary?, *Paleoceanography*, *17*(2), 1018, doi10.1029/2001PA000678, 2002.

Bralower, T. J., D. J. Thomas, J. C. Zachos, M. M. Hirschmann, U. Rhl, H. Sigurdsson, E. Thomas, and D. L. Whitney, High-resolution records of the late Paleocene thermal maximum and circum-Caribbean volcanism: Is there a link?, *Geology*, *25*, 963–966, 1997.

Crowley, T. J., and J. C. Zachos, Comparison of zonal temperature profiles for past warm time periods, in *Warm Climate in Earth History*, edited by B. T. Huber et al., Cambridge Univ. Press, New York, 2000.

Dickens, G. R., Methane oxidation during the Late Palaeocene Thermal Maximum, *Bull. Soc. Geol. Fr.*, *171*, 37–49, 2000.

Dickens, G. R., Carbon addition and removal during the late Paleocene thermal maximum: Basic theory with a preliminary treatment of the isotope record at Ocean Drilling Program Site 1051, Blake Nose, in *Western North Atlantic Paleogene and Cretaceous Paleoceanography*, edited by R. D. Norris et al., pp. 293–306, Geol. Soc. London, London, 2001.

Dickens, G. R., J. R. O'Neil, D. K. Rea, and R. M. Owen, Dissociation of oceanic methane hydrate as a cause of the carbon isotope excursion at the end of the Paleocene, *Paleoceanography*, *10*, 965–971, 1995.

Grenfell, J. L., D. T. Shindell, D. Koch, and D. Rind, Chemistry–climate interactions in the Goddard Institute for Space Studies general circulation model, 2, New insights into model-

ing the preindustrial atmosphere, *J. Geophys. Res.*, *106*, 33,435–33,451, 2001.
Hansen, J., M. Sato, and R. Ruedy, Radiative forcing and climate response, *J. Geophys. Res.*, *102*, 6831–6864, 1997.
Huber, M., and L. C. Sloan, Heat transport, deep waters, and thermal gradients: Coupled simulation of an Eocene Greenhouse Climate, *Geophys. Res. Lett.*, *28*, 3481–3484, 2001.
Hudson, T. L., and L. B. Magoon, Tectonic controls on greenhouse gas flux to the Paleogene atmosphere from the Gulf of Alaska accretionary prism, *Geology*, *30*, 547–550, 2002.
IPCC, *Climate Change 2001: The Scientific Basis*, Cambridge Univ. Press, New York, 2001.
Isaksen, I., and O. Hov, Calculations of trends in the tropospheric concentration of O_3, OH, CO, CH_4 and NO_x, *Tellus*, *39B*, 271–283, 1987.
Katz, M. E., D. K. Pak, G. R. Dickens, and K. G. Miller, The source and fate of massive carbon input during the latest Paleocene Thermal Maximum, *Science*, *286*, 1531–1533, 1999.
Katz, M. E., B. S. Cramer, G. S. Mountain, S. Katz, and K. G. Miller, Uncorking the bottle: What triggered the Paleocene–Eocene thermal maximum methane release?, *Paleoceanography*, *16*, 549–560, 2001.
Kennett, J., and L. D. Stott, Abrupt deep sea warming, paleoceanographic changes and benthic extinctions at the end of the Paleocene, *Nature*, *353*, 319–322, 1991.
Koch, P. L., J. C. Zachos, and P. Gingerich, Correlation between isotope records in marine and continental carbon reservoirs near the Palaeocene/Eocene boundary, *Nature*, *358*, 319–322, 1992.
Lacis, A. A., and V. Oinas, A description of the correlated k distribution method for modeling nongray gaseous absorbtion, thermal emission and multiple scattering in vertically inhomogeneous atmospheres, *J. Geophys. Res.*, *96*, 9027–9063, 1991.
Lashof, D. A., and D. R. Ahuja, Relative contributions of greenhouse emissions to global warming, *Nature*, *344*, 529–531, 1990.
Levy, H., Normal atmosphere large radical and formaldehyde concentrations predicted, *Science*, *173*, 141–143, 1971.
Norris, R. D., and U. Röhl, Carbon cycling and chronology of climate warming during the Palaeocene–Eocene transition, *Nature*, *401*, 775–778, 1999.
Oinas, V., A. A. Lacis, D. Rind, D. T. Shindell, and J. E. Hansen, Radiative cooling by stratospheric water vapor: Big differences in GCM results, *Geophys. Res. Lett.*, *28*, 2791–2794, 2001.
Pearson, and Palmer, Atmospheric carbon dioxide concentrations over the past 60 million years, *Nature*, *406*, 695–699, 2001.
Peters, R. B., and L. C. Sloan, High greenhouse gas concentrations and polar stratospheric clouds: A possible solution to high-latitude migration at the Latest Paleocene Thermal Maximum, *Geology*, *28*, 979–982, 2000.
Prather, M., et al., Atmospheric chemistry and greenhouse gases, in *Climate Change 2001: The Scientific Basis*, edited by J. T. Houghton et al., p. 881, Cambridge Univ. Press, New York, 2001.
Rind, D., M. Chandler, P. Lonergan, and J. Lerner, Climate change and the middle atmosphere, 5, Paleostratosphere in cold and warm climates, *J. Geophys. Res.*, *106*, 20,195–20,212, 2001.
Röhl, U., T. J. Bralower, R. D. Norris, and G. Wefer, New chronology for the late Paleocene thermal maximum and its environmental implications, *Geology*, *28*, 927–930, 2000.
Royer, D. L., S. L. Wing, D. J. Beerling, D. W. Jolley, P. L. Koch, L. J. Hickley, and R. A. Berner, Paleobotanical evidence for near present day levels of atmospheric CO_2 during part of the Tertiary, *Science*, *292*, 2310–2313, 2001.
Sander, S. P., et al., Chemical kinetics and photochemical data for use in stratospheric modeling, in *Eval. 13, JPL Publ.*, vol. 00-003, Jet Propul. Lab., Pasadena, Calif., 2000.
Shindell, D. T., and V. Grewe, Separating the influence of halogen and climate changes on ozone recovery in the upper stratosphere, *J. Geophys. Res.*, *107*(D12), 4144, doi:10.1029/2001JD000420, 2002.
Shindell, D. T., D. Rind, and P. Lonergan, Increased polar stratospheric ozone losses and delayed eventual recovery due to increasing greenhouse gas concentrations, *Nature*, *392*, 589–592, 1998.
Shindell, D. T., R. L. Miller, G. A. Schmidt, and L. Pandolfo, Simulation of recent northern winter climate trends by greenhouse-gas forcing, *Nature*, *399*, 452–455, 1999.
Shindell, D. T., J. L. Grenfell, D. Rind, C. Price, and V. Grewe, Chemistry–climate interactions in the GISS GCM, part 1, Tropospheric chemistry model description and evaluation, *J. Geophys. Res.*, *106*, 8047–8076, 2001a.
Shindell, D. T., G. A. Schmidt, R. L. Miller, and D. Rind, Northern Hemisphere winter climate response to greenhouse gas, ozone, solar and volcanic forcing, *J. Geophys. Res.*, *106*, 7193–7210, 2001b.
Sinha, A., and L. D. Stott, New atmospheric pCO_2 estimates from paleosols during the late Paleocene/early Eocene global warming interval, *Global Planet. Change*, *9*, 297–307, 1994.
Sloan, L. C., and D. Pollard, Polar stratospheric clouds: A high latitude warming mechanism in an ancient greenhouse world, *Geophys. Res. Lett.*, *25*, 3517–3520, 1998.
Sloan, L. C., and D. K. Rea, Atmospheric carbon dioxide and early Eocene climate: A general circulation modeling sensitivity study, *Palaeogeogr. Palaeoclimatol. Palaeoecol.*, *119*, 275–292, 1995.
Sloan, L. C., J. C. G. Walker, T. C. Moore, D. K. Rea, and J. C. Zachos, Possible methane induced warming in the early Eocene, *Nature*, *357*, 320–322, 1992.
Sloan, L. C., M. Huber, and A. Ewing, Polar stratospheric cloud forcing in a greenhouse world: A climate modeling sensitivity study, in *Reconstructing Ocean History*, edited by F. Abrantes and A. Mix, pp. 273–293, Kluwer Acad., Norwell, Mass., 1999.
Sze, N. D., Anthropogenic CO emissions: Implications for the atmospheric CO–OH–CH_4 cycle, *Science*, *195*, 673–675, 1977.
Thomas, D. J., T. J. Bralower, and J. C. Zachos, New evidence for subtropical warming during the late Paleocene thermal maximum: Stable isotopes from Deep Sea Drilling Project Site 527, Walvis Ridge, *Paleoceanography*, *14*, 561–570, 1999.
Zachos, J. C., D. Thomas, T. Bralower, and E. Thomas, New constraints on the timing and magnitude of the Paleocene–Eocene boundary carbon isotope excursion in marine environments, *Eos. Trans. AGU*, *82*, 767, Fall Meet. Suppl., 2001.

G. A. Schmidt and D. T. Shindell, National Aeronautics and Space Administration (NASA) Goddard Institute for Space Studies and Center for Climate Systems Research, Columbia University, 2880 Broadway, New York, NY 10025, USA. (gschmidt@giss.nasa.gov)